EXPERIMENTAL STUDY OF AN AXIAL VIRCATOR WITH RESONANT CAVITY

V. Baryshevsky, A. Gurinovich, E. Gurnevich, P. Molchanov

1. Introduction

Microwave devices with a virtual cathode attract many researches by the ability to operate without a guiding magnetic field, rather short operation region, enhanced tunability of the operation frequency, high output power, and relative simplicity of the resonator design [1–3]. However, low efficiency and instability of the generation frequency are typical disadvantages of most vircators.

The efficiency of vircators can be increased, particularly, by setting resonant conditions for the conversion of the beam energy into high-power microwaves. Different vircator designs with resonant cavities yave been analyzed both experimentally and numerically [6–9]. The studies of axial vircators with multicavity resonators prove the possibility of a resonant increase in the efficiency [10–12]. The authors of [12] have described the design of an axial vircator capable of power efficiency 6–7%. According to [12], the electron beam produced in a 630 kV, ~ 24 kA diode interacting with a multicavity resonator at a frequency of about 4 GHz provided the average output power of about 1 GW.

Numerical analysis of various configurations of axial vircators we made [13–18] yielded three designs of a multicavity resonator for an axial vircator, operating in the frequency range from 3 to 4 GHz with 400 keV electron beam and promising about 5% efficiency.

In the present paper, the experimental investigation of the axial vircator with the developed multicavity resonators is represented. The frequency and radiation power are analyzed for different cathodes and anode meshes and varied cathode-anode gaps.

2. System description

The developed axial vircator is driven by a pulsed power supply using a 30 kJ/100 kV capacitor bank and an exploding wire array (EWA) capable of generating a 600 kV voltage pulse. The EWA consists of parallel connected oxygen-free high-conductivity (OFHC) 99.99% purity copper wires 100 μm in diameter. The length and the number of wires can vary to match the EWA and vircator impedances. The EWA case is designed to be filled with gas (nitrogen or nitrogen and SF_6 mixture) at pressures up to 5 gauge atmospheres, but the array can also be fired in air. A pressurized SF_6 spark gap sharpens the high-voltage output, so that the diode voltage pulse approaching 400 kV with a rise time well below 100 ns is generated: the gas pressure and the gap between the electrodes can be varied.

The equivalent electrical scheme of the system is shown in Fig.1: marks 1, 2, and 3 indicate the location of three Rogowski coils.

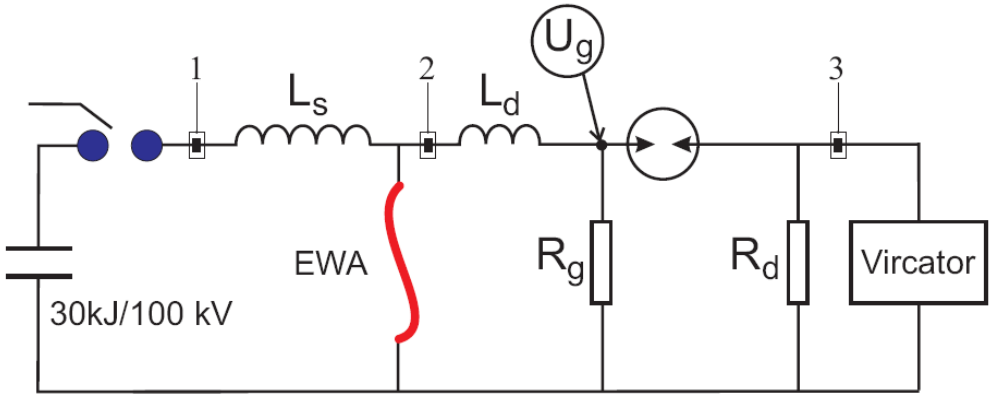

Fig.1. Equivalent electrical scheme of the system: location of three Rogowski coils are marked

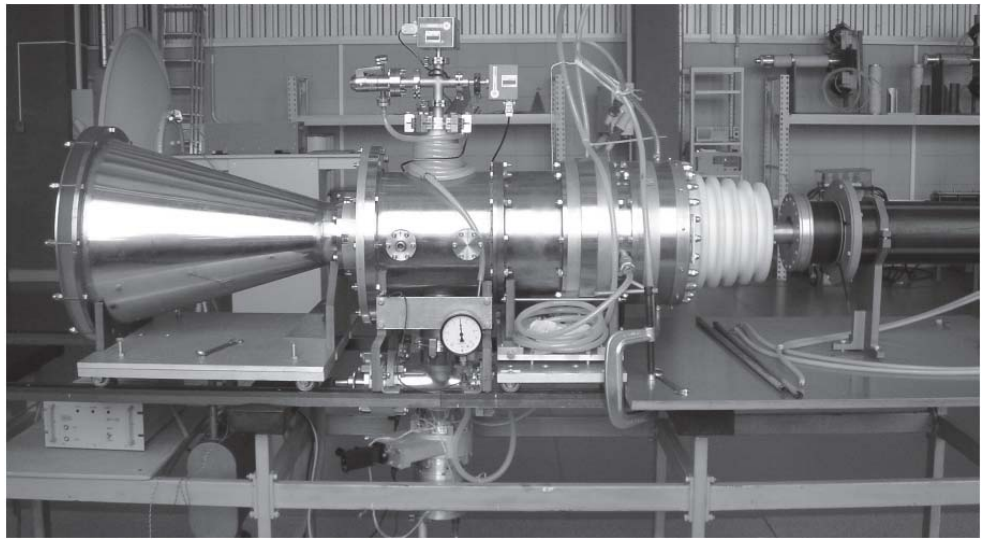

Fig. 2. System photo

Three designs of three-cavity resonators (see Fig.3 and Table 1) were considered in [14, 15] for an axial vircator operating in the frequency range from 3 to 4 GHz.

The operation of each design was simulated [14, 15] for a constant cathode voltage, ranging from 400 to 450 kV. The cathode parameters and the cathode-anode gap were determined so as to provide a stable generation and the highest possible values of the output power. The radiation frequency for the axial vircator with resonator #1 was predicted to be 3.2 GHz, and for systems #2 and #3, the expected radiation frequency was 3.6–3.7 GHz.

Resonators #1 and #2 are fabricated for the experimental study. They are housed in the drift tube, superposing the resonator output section with the horn input.

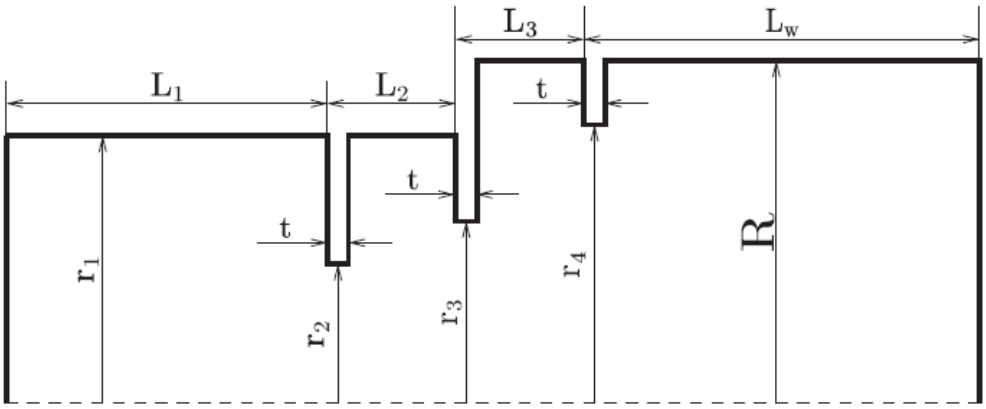

Fig. 3. Three cavity resonator geometry [15]

Table 1. Dimensions of three-cavity resonators (mm)

	L_1	L_2	L_3	L_w	r_1	r_2	r_3	r_4	R	t
#1	60	25	17	160	50	25	40	60	70	5
#2	54	26	20	160	45	25	33	37	50	5
#3	48	22	17	160	45	21	40	53	62	4

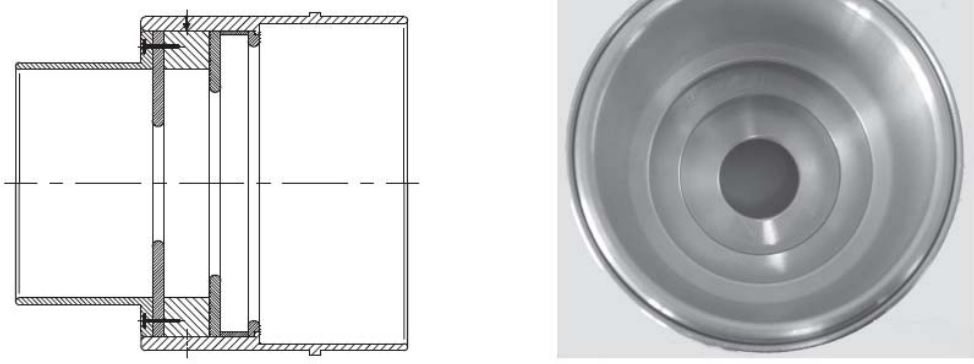

Fig. 4. Resonator drawing (left) and photo (right)

Stainless steel woven anode meshes with 77% and 91% geometric transparency are used in the experiments; the diameter of the mesh thread is 224 μm. The cathodes are made of dense fine-grained graphite MPG-8: solid and ring-type with outer diameters 50, 60, and 71 mm and different hatching.

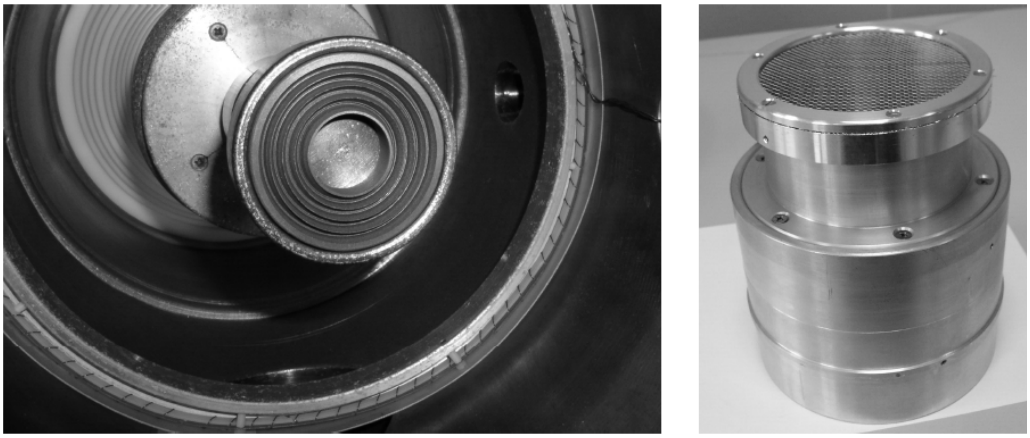

Fig. 5. Cathode installed on the cathode holder (left) and resonator with anode mesh (right)

Three Rogowski coils enable detecting the current derivatives in the system at points 1, 2, and 3 in Fig.1. Accurately measured inductances and resistances in the circuit allow evaluating the EWA voltage and the voltage applied to the cathode. The microwave emission is detected at a distance of 11.5 m from the horn output window by two receiving antennas Geozondas 1 – 4.5 GHz and Tektronix oscilloscopes TDS7704 and TDS7354. All the measuring channels are synchronized.

3. Experimental results

The experimental investigation of an axial vircator with multicavity resonator is intended to ascertain the system parameters providing stable, single-frequency, high-power microwave generation. The typical voltage and current signals obtained for EWA containing 20 wires of 700 mm length are presented in Fig. 6. Two peaks emerge on the voltage curve: the first one (left) corresponds to spark gap closing and the second (right) marks the maximum diode voltage. The diode current value correlates with that in the simulation [15].

The sample of the detected microwave signal and its spectral content obtained by the short-time Fourier transform are shown in Fig.7. All the signals are synchronized. Knowing the gain and directivity of the system output horn and the parameters of the receiving antenna, we can convert the electric field strength measured at a certain distance from the output window to the radiated power.

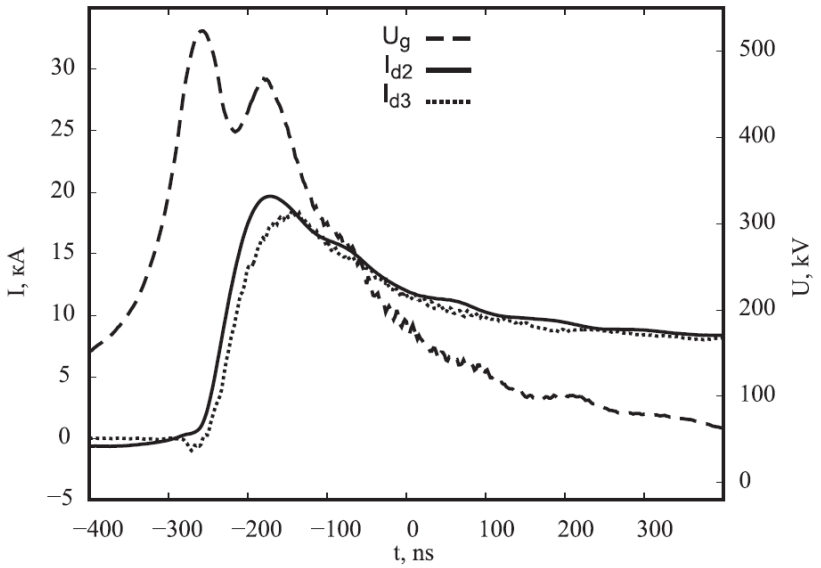

Fig. 6. Evaluated voltage U_g and diode current measured by sensors 2 and 3 (see Fig.1)

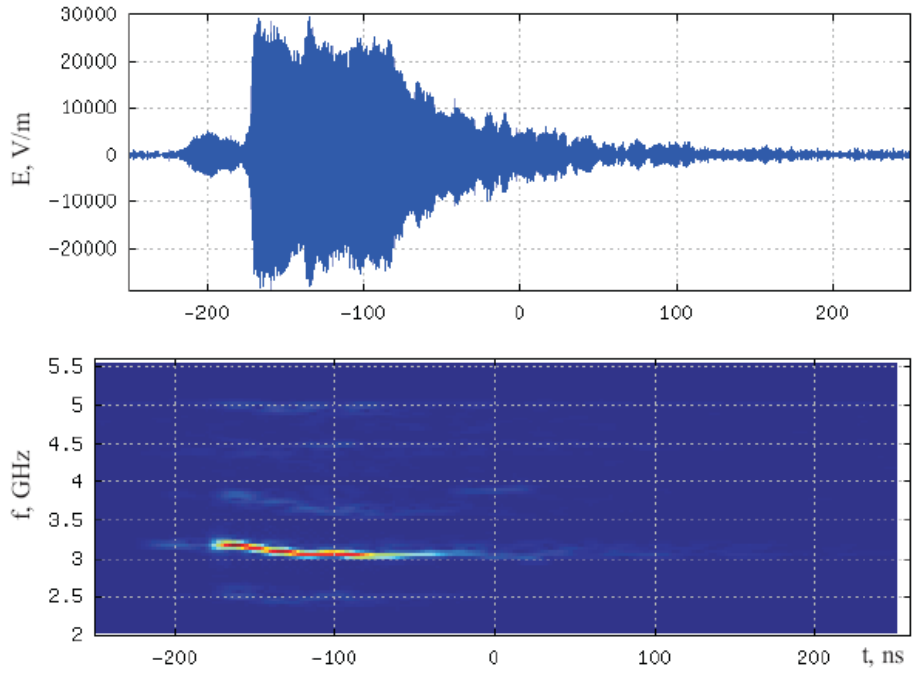

Fig. 7. Detected microwave signal and its spectral content obtained by the short-time Fourier transform

The simulation results [15] are used as a guideline. When selecting what parameter is to be tuned, we analyzed the operation frequency, the microwave pulse duration and amplitude, as well as the correlation between microwave and current pulses.

Resonator #1

According to the simulation [15], at the cathode voltage of 450 kV and the cathode-anode gap $h = 14$ mm, the peak power reaches 700 MW at 3.2 GHz. In the experimentally obtained spectrum for the solid cathode with outer diameter of 60 mm at $h = 14$ mm, two frequencies are present (see the upper spectrum in Fig.9). The radiation frequency grows with decreasing beam current and voltage, and the radiated peak power is as low as 70 MW. The radiation frequency changes with the cathode-anode gap value change as shown in Fig. 8. This behavior is in harmony with the simulation of radiation spectra for different beam impedance values (see [16]): when the cathode-anode gap is reduced (i. e., the beam impedance is reduced) to appear below a certain value, the basic vircator frequency grows. This is due to an increase of the electron beam plasma frequency [4, 5].

With the cathode-anode gap h varying from 13 to 17 mm, the diode current pulse, the microwave pulse duration, and the peak power remain almost the same; but further increase of h leads to power reduction and the microwave pulse delay with respect to the current pulse. Finally, the cathode-anode gap value $h = 16$ mm is selected for later experiments.

The increase of the solid cathode diameter to 71 mm gives $\sim 50\,\%$ gain in the microwave signal amplitude Fig.10 (peak power is about 120 MW).

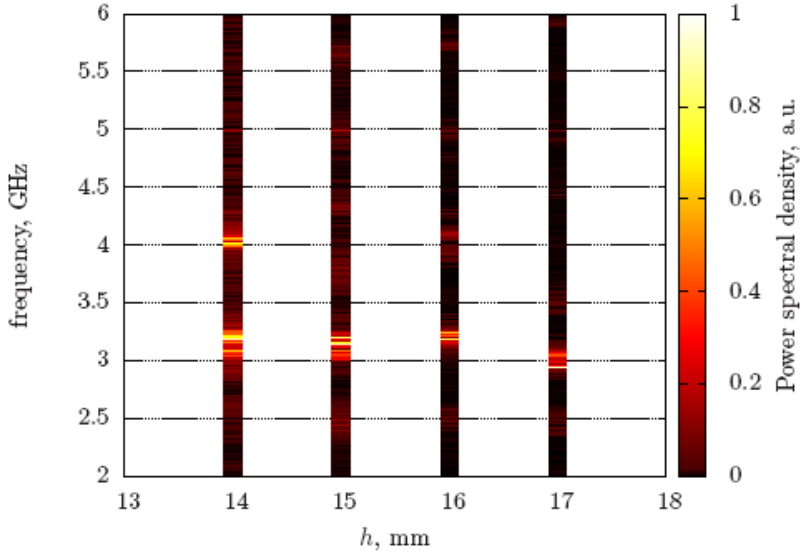

Fig. 8. Comparison of spectra obtained for different cathode-anode gap values. The increase of the cathode-anode gap provides a suppression of the higher frequency in the spectrum and results in a single-frequency generation (see the lower spectrum in Fig.9 obtained for the same cathode at h = 17 mm)

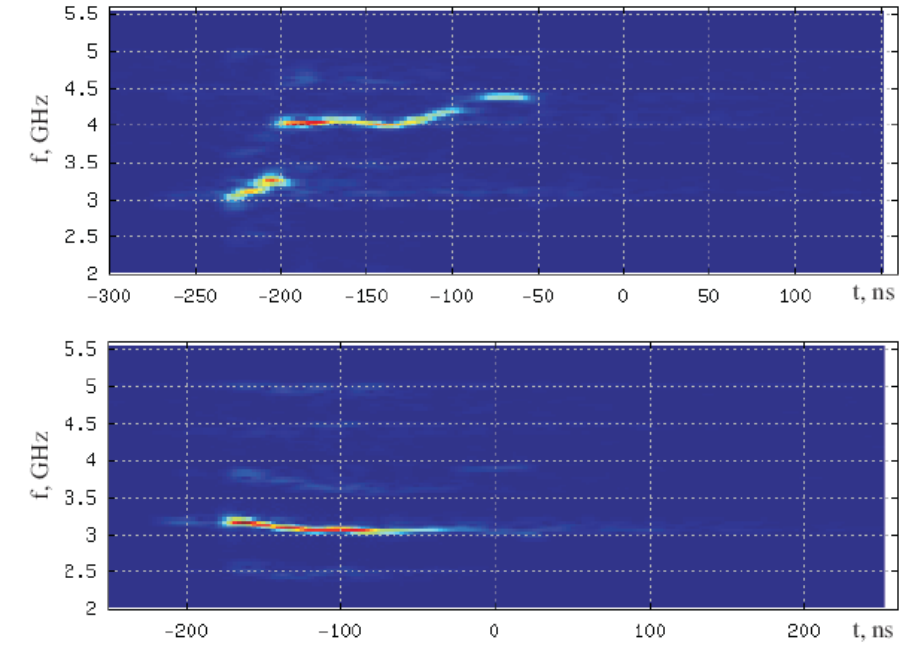

Fig. 9. Spectrogram of the microwave signal obtained for h = 14 mm (upper) and h = 17 mm (lower)

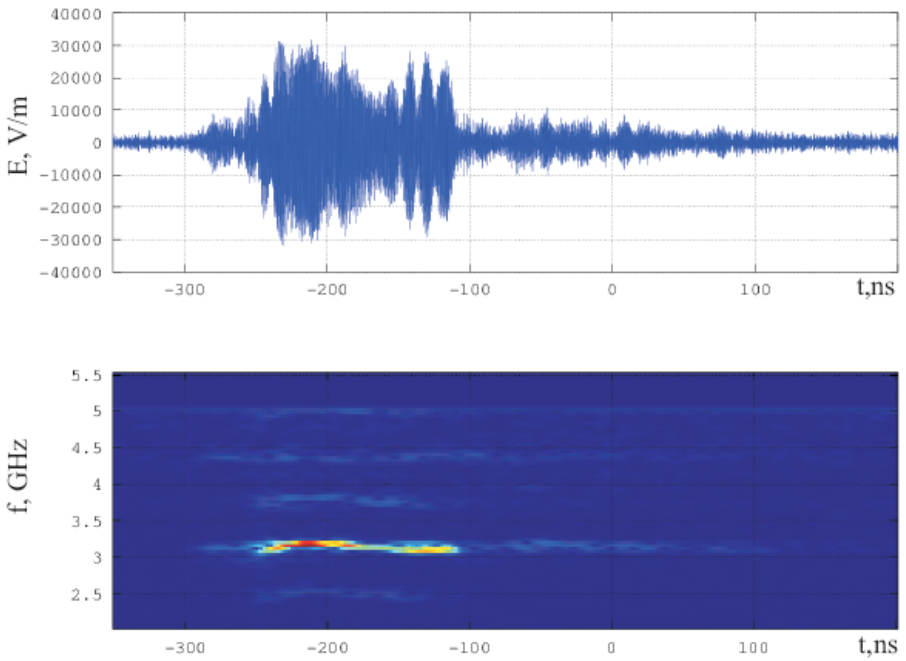

Fig. 10. Detected microwave signal and its spectrogram for the solid cathode with outer diameter 71 mm and cathode-anode gap h = 16 mm

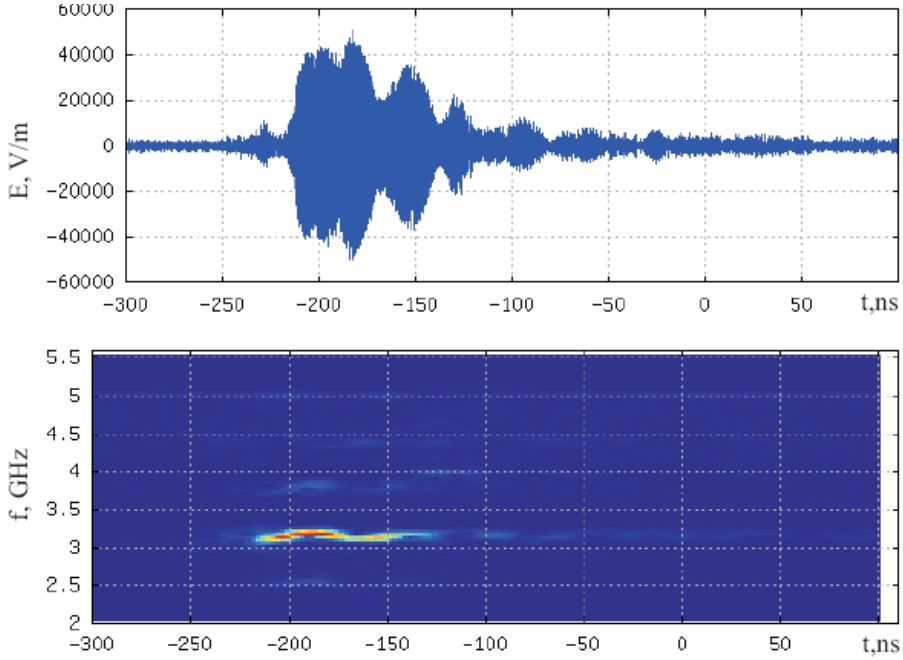

Fig. 11. Detected microwave signal and its spectrogram for the ring-type cathode with outer diameter 60 mm, inner diameter 24 mm, and cathode-anode gap h = 16 mm

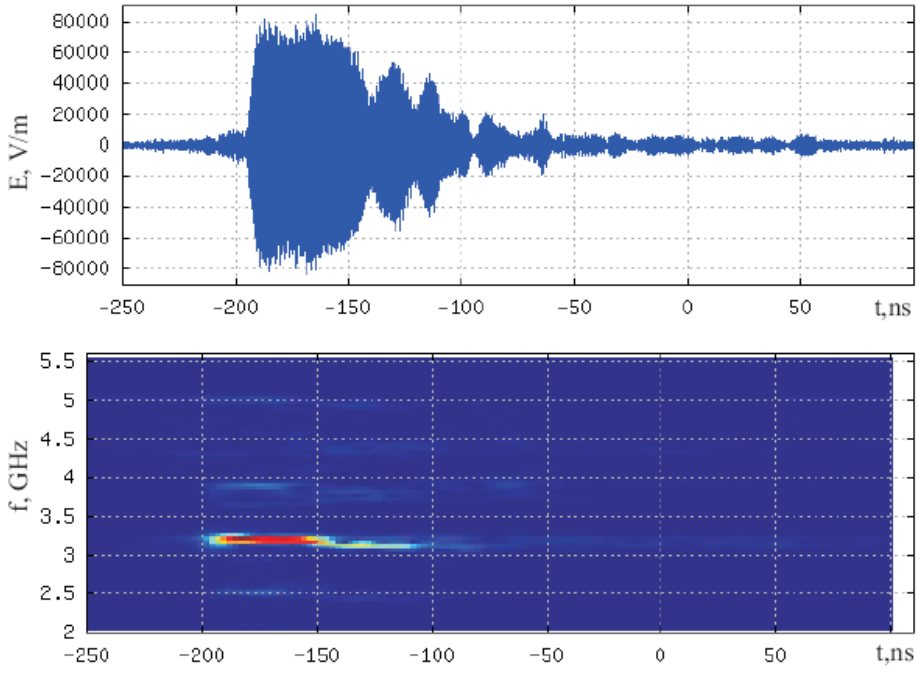

Fig. 12. Detected microwave signal with the highest amplitude and its spectrogram for the ring-type cathode with outer diameter 60 mm, inner diameter 24 mm, and cathode-anode gap h = 16 mm

The study of the ring-type cathodes with outer diameter of 60 mm enables us to achieve the peak power values close to those predicted in [15]. The progressive enlargement of the cathode inner diameter from 20 to 24 mm, when keeping all other parameters the same, results in an increase of the peak radiated power to 300 MW (Fig.11) and even to 600 MW in several shots (Fig.12).

The microwave signal decreases at the cathode inner diameters greater than 24 mm.

The comparison of the simulation results [15] and the data obtained experimentally demonstrates a perfect fit in the basic frequency and accordance in the radiated power (see Fig.13)

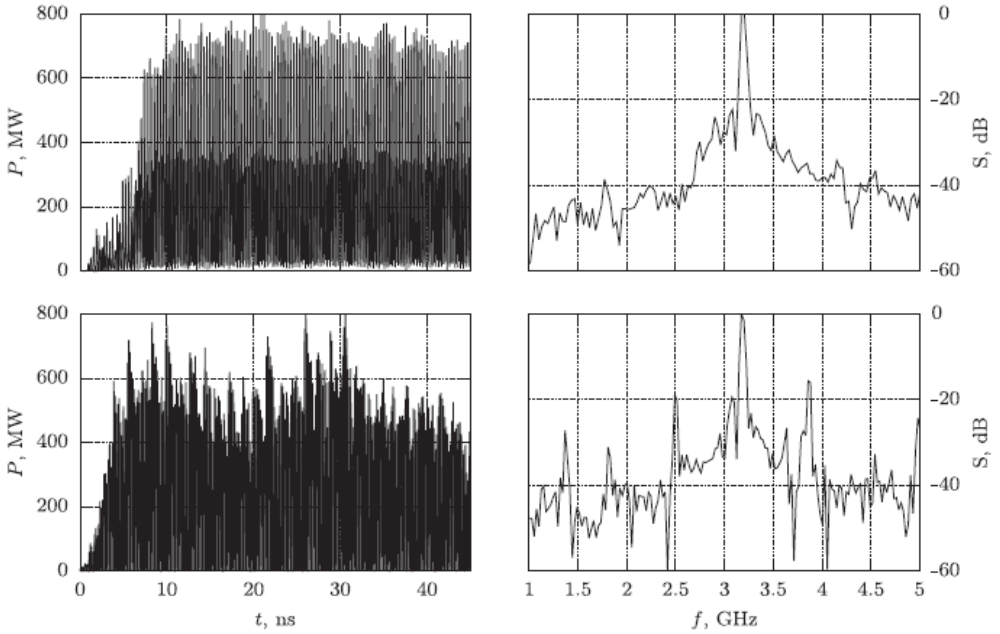

Fig. 13. Comparison of simulation results [15] (upper pictures) and data obtained experimentally (lower pictures) for ring-type cathode with outer diameter 60 mm, inner diameter 24 mm, and cathode-anode gap h = 16 mm

Resonator #2

According to the simulation [14, 15], for resonator #2, a stable generation with instantaneous peak power of about 800 MW at the frequency of 3.6 GHz can be obtained.

Performing similar series of experiments, we also managed to find the set of the system parameters for resonator #2 (solid cathode with outer diameter 60 mm and cathode-anode gap 14 mm) stably providing the microwave output as high as 200 MW at the frequency ~3.6 GHz (see Fig.14). However, occasional shots with higher power are also observed. The voltage pulse and diode current are the same as in Fig.6.

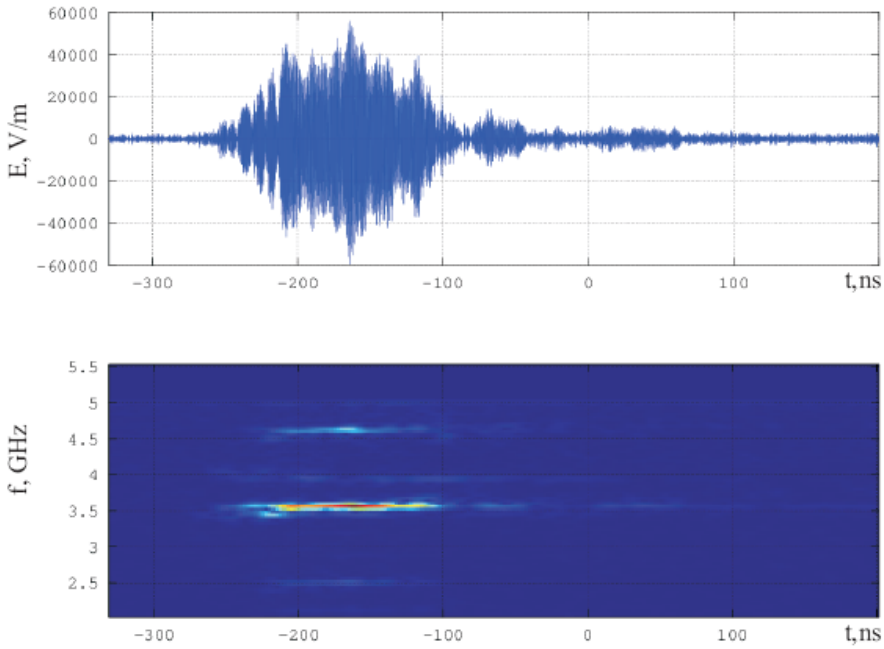

Fig. 14. Detected microwave signal and its spectrogram for resonator #2 with a solid cathode with outer diameter 60 mm and cathode-anode gap h = 14 mm

Use of the ring-type cathodes and the cathodes with a diameter other than 60 mm for this case gives no benefit. The increase in the cathode-anode gap is destructive for both single-frequency generation and power level.

4. Conclusion

Multicavity resonators for an axial vircator have been developed and experimentally investigated. The frequency and radiation power have been analyzed for two different resonator designs. The influence of the cathode-anode gap, the cathode shape and size have been considered.

However, the results with the highest power appeared to be poorly reproducible, though the parameters of the system and the records in the utmost and ordinary cases seem to be identical. We associate the observed instability of the results with the features of the electron beam, particularly, the homogeneity of electron emission from the cathode surface and momentum (energy) spread. According to simulation of the axial vircator with multicavity resonators [16], when the momentum (energy) spread is increased from 1% to 5%, the efficiency drops from 6% to ~1%. Different variants of cathode hatching have been tested to ensure a homogeneous emission from the cathode surface. The effectiveness of this approach has been confirmed experimentally, but to get a sustained result, a thorough analysis of the cathode-anode gap geometry and the electron beam dynamics is required. In addition, an extremely fast damage of the anode

mesh in the experiments with the ring-type cathodes, in contrast to the experiments with solid cathodes, remains to be explained.

The anode mesh with higher transparency gives no advantages; moreover, additional efforts are needed to retrieve the impedance matching by changing the EWA parameters. Perhaps, anode meshes made of different materials could contribute to the momentum spread decrease.

All the above questions initiate simulation of explosive-emission and electron beam dynamics in a cathode-anode gap for cathode and anode optimization in an axial vircator [18].

Acknowledgment

The authors would like to thank Victor Evdokimov for the sophisticated system design and Nikolai Belous for permanent involvement in the experimental activities.

References

1. *Miller R. B.* An Introduction to the Physics of Intense Charged Particle Beams; Springer US, 1982
2. *GranatsteinV. L., Alexeff I.* High Power Microwave Sources. Boston, MA: Artech House, 1987
3. *Benford J., Swegle J. A. , Schamiloglu E.* High Power Microwaves. Second Edition, 2007
4. *Didenko A. N. , Fomenko G. P., Gleizer I. Z. et al.* //Proc. of the 3rd International Topical conference on High Power Electron and Ion Beam. Novosibirsk. 1979. Vol. II. P. 683–691
5. *Sullivan D. J.* // IEEE Trans. on Nuclear Sci. 1983. Vol. NS-30, no. 4. P. 3426–3428
6. *Jiang W., Shimada N., Prasad S. D., Yatsui K.* // IEEE Trans. Plasma Sci. 2004. Vol. 32, No. 1. P. 54–59
7. *Kitsanov S. A., Klimov A. I., Korovin S. D. et al.* //IEEE Trans. Plasma Sci. 2002. Vol. 30 P. 1179–1185
8. *Didenko A. N., Gorbachev K. V., Kogutnitskii A.E. et al.* // Proc. of 11th International Conference on High-Power Particle Beams. 1996. Vol. 1. P. 445-448
9. *Champeaux S., Gouard P., Cousin R., Larour J.* // Proc. of 14th International Vacuum Electronics Conference (IVEC2013). doi:10.1109/IVEC.2013.6571105
10. *Liu Z., Shu T., Zhang J., Qian B.* //Plasma Science & Technology. 2003. Vo1.5, No.5 P. 2006–2010
11. *Shu T., Wang Y., Qian B., Tan Q.* // Chin. Phys. Lett. 2002. Vol. 19, No. 11. P. 1646–1649
12. *Li Z., Zhong H., Fan Y. et al.* // Chin. Phys. Lett. 2008. Vol. 25, No. 7. P. 2566–2569
13. *Baryshevsky V., Gurinovich A., Molchanov P., Anishchenko S., Gurnevich E.*// IEEE Transactions on Plasma Science. 2013. Vol. 41, issue 10. P. 2712–2716
14. *Gurnevich E.A., Molchanov P.V.*// IEEE Trans. Plasma Sci. 2015. Vol. 43, issue 4. P. 1014–1017
15. *Molchanov P.V. , Gurnevich E. A., Tikhomirov V. V., Siahlo S. E.* Simulation of an axial vircator with a three-cavity resonator. arXiv:1408.1824
16. *Anishchenko S., Gurinovich A.* // J. of Physics: Conf. Ser. 2014. Vol. 490. P. 012116
17. *Anishchenko S. V., Gurinovich A.* // Comput. Sci. Disc. 2014. Vol. 7. P. 015007
18. *Anishchenko S., Gurinovich A.* // Proc. EAPPC2014. P. OA1-5